HHS Public Access

Author manuscript

Prog Neurobiol. Author manuscript; available in PMC 2024 December 01.

Published in final edited form as:

Prog Neurobiol. 2023 December ; 231: 102531. doi:10.1016/j.pneurobio.2023.102531.

Neuronal plasticity contributes to postictal death

Anastasia Brodovskaya[1], **Huayu Sun**[1], **Nadia Adotevi**[1], **Ian C. Wenker**[2], **Keri E. Mitchell**[3], **Rachel T. Clements**[4], **Jaideep Kapur**[1,5]

[1]Department of Neurology, University of Virginia, Charlottesville, VA 22908 USA

[2]Department of Anesthesiology, University of Virginia, Charlottesville, VA 22908 USA

[3]Department of Chemistry, University of Virginia, Charlottesville, VA 22908 USA

[4]Department of Neuroscience, University of Virginia, Charlottesville, VA 22908 USA

[5]UVA Brain Institute, University of Virginia, Charlottesville, VA 22908 USA

Abstract

Repeated generalized tonic-clonic seizures (GTCSs) are the most critical risk factor for sudden unexpected death in epilepsy (SUDEP). GTCSs can cause fatal apnea. We investigated neuronal plasticity mechanisms that precipitate postictal apnea and seizure-induced death. Repeated seizures worsened behavior, precipitated apnea, and enlarged active neuronal circuits, recruiting more neurons in such brainstem nuclei as periaqueductal gray (PAG) and dorsal raphe, indicative of brainstem plasticity. Seizure-activated neurons are more excitable and have enhanced AMPA-mediated excitatory transmission after a seizure. Global deletion of the GluA1 subunit of AMPA receptors abolishes postictal apnea and seizure-induced death. Treatment with a drug that blocks Ca^{2+}-permeable AMPA receptors also renders mice apnea-free with five-fold better survival than untreated mice. Repeated seizures traffic the GluA1 subunit-containing AMPA receptors to synapses, and blocking this mechanism decreases the probability of postictal apnea and seizure-induced death.

Graphical Abstract

Correspondence to: Jaideep Kapur, MD, PhD, UVA Brain Institute, University of Virginia, Health Sciences Center, P.O. Box: 801330, Charlottesville, VA 22908 USA, jk8t@virginia.edu.

Author contributions

A.B., H.S., J.K. conceived, designed experiments and wrote the manuscript. A.B. did apnea, 3D reconstruction, and IEM experiments. H.S. performed patch-clamp recordings. N.A. carried out kindling experiments. I.W. assisted with plethysmography chamber construction and setup. K.M. and R.C. helped with data analysis and i.p. injections.

Competing interests

The authors report no competing interests.

Declaration of interests

The authors declare that they have no known competing financial interests or personal relationships that could have appeared to influence the work reported in this paper.

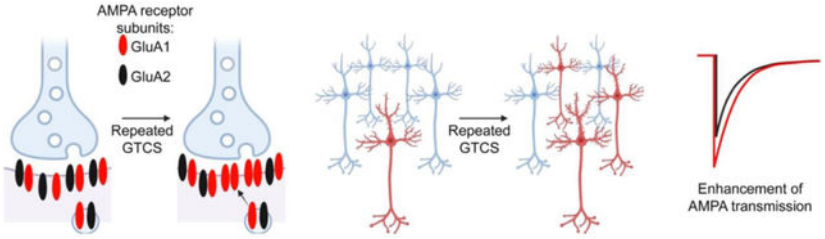

Keywords

SUDEP; epilepsy; seizures; apnea; brainstem plasticity; GluR1 subunit; AMPA

Introduction

Repeated generalized tonic-clonic seizures (GTCSs) are the single most significant risk factor for SUDEP, which is the sudden, unexpected, witnessed or unwitnessed, non-traumatic and non-drowning death of patients with epilepsy, with or without evidence of a seizure and excluding status epilepticus (Nashef, 1997; Nashef et al., 2012). A nationwide epidemiological study of SUDEP in Sweden further confirmed repeated GTCSs were a leading risk factor for SUDEP (Sveinsson et al., 2020). In other studies, repeated GTCSs were the leading risk factor for SUDEP as well (Devinsky et al., 2016; Harden et al., 2017; Hesdorffer et al., 2011; Tomson et al., 2008).

Several studies suggest that apnea occurs following GTCS and may be fatal. It was previously believed that SUDEP is due to cardiac mechanisms, yet in the famous MORTEMUS study, the largest study of SUDEP cases that occurred in Epilepsy Monitoring Units, terminal postictal apnea always preceded terminal asystole (Ryvlin et al., 2013). The NIH-funded SUDEP Center Without Walls confirmed these findings in a prospective study. The group observed post-convulsive apnea in two patients with near-SUDEP and one with probable SUDEP, suggesting that postictal apnea is a clinical biomarker of SUDEP (Vilella et al., 2019). Similar evidence comes from animal models, where seizure-induced respiratory dysfunction is critical, and genetic mutations lead to severe epilepsy and SUDEP (Massey et al., 2014; Teran et al., 2022). Leading investigators have proposed that seizures may invade the brainstem and cause apnea (Faingold, 2012; Kim et al., 2018; Kommajosyula et al., 2017; Patodia et al., 2018; Petrucci et al., 2020; Teran et al., 2022; Wengert et al., 2021; Xia et al., 2022; Zhang et al., 2018). Seizure spread through the forebrain or amygdala connections is also thought to influence brainstem neurons (Teran et al., 2022). Although seizure activation of the brainstem has been demonstrated (Kommajosyula et al., 2017; Wengert et al., 2021; Xia et al., 2022), whether seizure repetition causes brainstem plasticity changes is unknown. Specifically, the precise plasticity mechanisms that cause apnea are unclear.

AMPA receptor plasticity plays a critical role in learning and memory. Motor learning increases trafficking of AMPA receptors (AMPARs) containing GluA1 subunit into spines as shown by two photon *in vivo* imaging (Roth et al., 2020). Classical, tetanus-induced long-term potentiation (LTP) in hippocampal synapses also depends on AMPAR containing

GluA1 subunit (Shimshek et al., 2017). We previously demonstrated that mice with self-sustaining status epilepticus have enhanced synaptic surface expression of GluA1 subunit-containing AMPA receptors (Joshi et al., 2017). Because hippocampal neurons undergo plasticity changes during status epilepticus, we conditionally knocked down GluA1 subunit in excitatory hippocampal neurons, rendering status epilepticus less severe and shorter, which indicates the GluA1 subunit plays a critical role in sustaining status epilepticus (Adotevi et al., 2020). Studies of hypoxia-induced seizures in neonates also demonstrate AMPA receptor potentiation (Rakhade et al., 2008).

Here, we propose that increased excitatory transmission plasticity mediated by AMPA receptors, specifically through the GluA1 subunit, is critical for apnea and seizure-induced death.

Results

Seizure worsening and apnea development are forms of plasticity that result from repeated seizures

We plotted the published human SUDEP data from a combined analysis of four studies from the US, Scotland, and Sweden that demonstrated a tight correlation ($R^2 = 0.85$) between the number of generalized tonic-clonic seizures (GTCSs) and the risk of death (odds ratio) (Hesdorffer et al., 2011) (Fig. 1A). We induced repeated GTCSs in C57BL/6 mice using pentylenetetrazole (PTZ, 50 mg/kg, i.p.) every other day for the total of 10 seizures to model repeated GTCSs in humans (Fig. 1B). Repeated GTCSs increased the risk of seizure-induced death similar to human studies: 41.2% of mice died by the 10^{th} GTCS (Fig. 1C).

The second element of human SUDEP, according to the MORTEMUS study (Ryvlin et al., 2013), is that postictal terminal apnea occurs before terminal asystole. To determine if our mouse model had this second characteristic feature of human SUDEP, we recorded EEG, breathing, and EKG (Fig. 1B), by implanting two bilateral subdural frontal lobe EEG electrodes and an electrocardiogram lead (ECG). We monitored PTZ-injected individual mice (n = 17) with video, EEG, and ECG in a custom-made plethysmography chamber to record breathing (Wengert et al., 2021). The apnea region was defined as at least half of the baseline amplitude breathing recording with > 1 s interbreath interval. During initial seizures, mice had brief ictal apnea (2.68 ± 0.14 s) but no postictal apnea (Fig. 1E,H). With repeated seizures, some mice gradually developed postictal apnea (19.29 ± 5.04 s) followed by recovery (Fig. 1F) and subsequently had terminal postictal apnea (Fig. 1H). In contrast, others died at the first postictal apnea (Fig. 1H), which indicated that postictal apnea could be a biomarker to predict death. All mice that died always had postictal apnea followed by progressive bradycardia (Fig. 1G), and apnea always occurred before death ($R^2 = 0.84$, Fig. 1D,H). Because repeated GTCSs gradually lead to apnea, it is a novel form of kindling-like plasticity.

Repeated GTCSs progressively worsen in severity and have a faster onset. To scale seizure behavior, we used a modified Racine scale, where stage 5 seizures characterized rearing and falling, while stage 6 were wild running and involuntary jumping (Lewczuk et al., 2018).

No mice receiving 50 mg/kg PTZ had status epilepticus (seizures lasting longer than 5 min) or seizure clusters. Behavioral seizures worsened with repetition and became more intense (Fig. 1I); at least one stage 6 seizure occurred in 71% of mice by the 10th GTCS (Fig. 1J). Fatal seizures were significantly longer than 1st seizure, whereas nonfatal 10th seizures were of the same duration as the 1st seizures (mice that survived: 1st seizure 20.22 ± 1.77, 10th seizure 19.80 ± 1.32 s, paired t-test, n.s. p = 0.86; mice with fatal seizures: 1st seizure 18.57 ± 1.45, fatal seizure 25.43 ± 1.96 s, paired t-test, p = 0.020). All mice exhibited postictal generalized suppression after seizures. Latency to seizure onset decreased with repetition from 5.35 ± 0.9 min for the 1st seizure to 2.9 ± 0.4 min for the 10th seizure (Fig. 1K). Worsened seizure severity and apnea occurrence are forms of plasticity that repeated seizures gradually develop, which subsequently lead to death.

Seizure repetition increased brainstem activation

Although it has been previously reported that seizures invade brainstem networks (Kommajosyula et al., 2017; Wengert et al., 2021; Xia et al., 2022; Zhang et al., 2018), which might affect breathing, whether seizures alter brainstem activity with repetition is unclear. We compared neuronal activation changes in the brainstem after repeated seizures versus after only one seizure. To visualize activated neurons, we used targeted recombination in active population (TRAP2) mice (Allen et al., 2017; Guenthner et al., 2013). In these mice, activity-dependent c-Fos promoter drives Cre-ER expression. Injection of 4-hydroxytamoxifen (4-OHT) within 90 min of a seizure translocates Cre into the nucleus and causes tdTomato protein expression to label activated neurons. We have previously confirmed that these mice do not have leaky Cre expression (Naik et al., 2021). One group of TRAP2 mice received 4-OHT injection after repeated GTCSs on the first stage 6 seizure (n = 5 mice, Fig. 2A), while the control group received 4-OHT after a single stage 5 seizure (n = 4 mice, Fig. 2B). We built a 3D brainstem reconstruction map by stacking brain slices in the NeuroInfo software, using the same number of slices between each brain region in both groups (Fig. 2C). We found the most obvious increased neuronal activation in the dorsal raphe (59.8 ± 6.0 vs 39.3 ± 4.5, unpaired t-test, p = 0.016) and periaqueductal gray (PAG) (237.6 ± 16.1 vs 158.0 ± 7.8 cells, unpaired t-test, p = 0.0021) and compared to mice that only had one seizure (Fig. 2G). Our current studies continue sampling other brainstem regions.

We next wondered if repeated seizures activate the same neurons as the first seizure and expand the map or whether repeated seizures activate neurons randomly. To label two seizures separately, we injected TRAP2 mice with 4-OHT after the first seizure (red TdTomato neurons), and five days later (time necessary for tdTomato expression), we induced a second similar seizure, perfusing mice (n = 4) within 90 min and immunolabeling for c-Fos or ARC (green). Because the motor cortex generates generalized tonic-clonic seizures (Hughlings Jackson, 1890), we quantified neuronal overlap there. Surprisingly, repeated seizures activate the same neurons as the initial seizures and expand the network recruiting more neurons (Fig. 2D–F). 95% of all neurons active during the first seizure were also active during the second. Therefore, seizures repeat and expand the activation map. Enhanced neuronal activation with seizure repetition in the brainstem nuclei is a kindling-like phenomenon (Fig. 2H). These activity changes could also result from plasticity, or

enhanced interneuronal activation in response to increased excitability or enhanced neuronal firing in response to hypoxia/hypercapnia.

Seizure-activated neurons are more excitable than nonactive surrounding neurons

We next wanted to determine the cellular basis of the plasticity in seizure-activated neurons. Hughlings Jackson proposed that the motor cortex generates generalized tonic-clonic seizures (Hughlings Jackson, 1890), which Wilder Penfield confirmed (Penfield and Jasper, 1954). Our previous studies also showed dendritic spine enlargement in hippocampal pyramidal neurons after a single seizure (Naik et al., 2021), so we performed patch-clamp recordings on the pyramidal neurons of the motor cortex. Although the motor cortex participates in voluntary breathing, the exact neuronal circuits that lead to apnea are unclear. However, here, we focused on the molecular changes in activated neurons after a single seizure, so we compared the electrophysiological properties of seizure-activated and non-active surrounding neurons to determine whether activated neurons are more excitable than non-activated surrounding neurons. To quickly label seizure-activated neurons, we used transgenic c-Fos GFP mice instead of TRAP2 mice. These mice rapidly express eGFP under the control of the c-Fos promoter in activated neurons (within 30 min of a seizure) (Naik et al., 2021; Reijmers et al., 2007). GFP is not expressed as long as the mice are maintained on a diet containing doxycycline, which acts on the Tet repressor element. When c-Fos GFP mice are removed from a doxycycline diet 48 hrs before GTCS, c-Fos promoter in the activated neurons drives tetracycline-transactivator (tTA) that allows rapid GFP expression (Naik et al., 2021; Reijmers et al., 2007). We prepared coronal motor cortical slices and identified activated neurons (eGFP tagged) and nonactive surrounding neurons (untagged) based on eGFP expression under a fluorescent/DIC microscope (Fig. 3A). We confirmed pyramidal neuron identity by checking their firing properties, filling them with biocytin, and conducting a morphological analysis (Fig. 3B).

We first verified that tagged and untagged neurons have similar passive membrane properties after a single seizure (5 tagged layer 2/3 pyramidal neurons, 8 surrounding untagged pyramidal neurons, n = 5 mice, 1 hr after a GTCS). Tagged and untagged neurons had similar rest membrane potential ($p = 0.480$, paired t-test, Fig. 3C), membrane time constant (which reflects the size of neuronal surface area and is a function of membrane resistance and capacitance, $p = 0.407$, Fig. 3D), and membrane resistance ($p = 0.514$, Fig. 3E).

To test active membrane properties, we applied a series of current steps from −60 mV membrane potential. The action potential (A.P.) threshold in tagged neurons was lower and closer to the resting membrane potential compared to untagged neurons (tagged: −47.47 ± 3.26 mV, untagged: −39.30 ± 2.89 mV, $p = 0.046$, paired t-test, Fig. 3F). The A.P. amplitude and width were similar ($p = 0.252$ and $p = 0.463$ respectively, Fig. 3G,H). The lower A.P. threshold of tagged neurons suggests that they had higher excitability. To confirm it, we analyzed the relationship between membrane resistance and rheobase current (the minimum current that will produce an action potential). The membrane resistance was similar, but the rheobase current was lower in tagged cells ($p = 0.213$ for $R_{membrane}$, $p = 0.006$ for rheobase, Fig. 3I).

Tagged neurons fired more action potentials in response to depolarizing steps than untagged neurons, as confirmed by plotting the current step versus action potential frequency curve for each group (Fig. 3J,K). Spikes were more frequent in response to current injection in tagged neurons compared to untagged neurons (F-I plot, $p < 0.0001$, two-way ANOVA, Fig. 3L). There was a higher spike frequency in the first 10 A.P.s observed in tagged neurons compared to untagged neurons (Fig. 3M). In summary, tagged neurons were more excitable than surrounding untagged neurons, showing a lower threshold and more action potentials in response to depolarization.

Seizure-activated neurons demonstrate increased AMPA transmission

Because AMPA receptor plasticity is critical for learning and memory(Ge and Wang, 2021; Roth et al., 2020), we compared AMPA receptor-mediated spontaneous excitatory postsynaptic currents (sEPSCs) of layer 2/3 pyramidal seizure-tagged and untagged neurons, using voltage-clamp recordings and blocking GABA-A receptors and NMDA receptors(Rajasekaran et al., 2012, 2010). We found that AMPA receptor-mediated sEPSCs occurred more frequently in tagged neurons than untagged neurons after a single seizure (0.519 ± 0.345 Hz vs. 0.947 ± 0.459 Hz, $p = 0.042$, K.S. test, Fig. 3N). The amplitude of sEPSCs was larger in a tagged neuron than that recorded from an untagged neuron (18.27 ± 6.06 mV vs. 22.73 ± 6.14 mV, $p = 0.034$, K.S. test, Fig. 3O,P). We confirmed this finding in 13 tagged and 16 surrounding untagged neurons from 12 animals.

Interestingly, amplitudes of sEPSCs recorded from untagged neurons were normally distributed and fit a single Gaussian function with a mean amplitude of 16.87 ± 3.69 pA, which indicated there was one quantal release (Fig. 3Q). In contrast, the sEPSCs amplitude distribution histograms of tagged neurons were not normally distributed and fit two Gaussian distributions (two populations) with the mean of 20.84 ± 6.41 pA for the first population and 36.13 ± 11.89 pA for the second population, which indicated there were two quantal releases (Fig. 3R). The rise time and decay of sEPSCs recorded from tagged and untagged neurons were similar ($p = 0.919$ and $p = 0.654$ respectively, K.S. test, Fig. 3S,T), which suggested that the binding kinetics of AMPA receptors were similar in the two groups. In summary, tagged neurons were more excitable and had more frequent and larger AMPA receptor-mediated sEPSCs than untagged neurons.

Deletion of the GluA1 subunit of AMPA receptors decreases the probability of apnea and seizure-induced death

Enhanced AMPA-mediated currents in activated neurons indicate AMPA receptor plasticity during seizures. Activity-mediated trafficking of the GluA1 subunit of AMPA receptors, specifically to synaptic surface is well documented in long-term potentiation (LTP) and motor learning (Fortin et al., 2010; Malinow, 2003; Miyamoto et al., 2021; Patterson et al., 2010). Our previous work in animals with self-sustaining status epilepticus demonstrated that the synaptic surface expression of GluA1 subunit-containing AMPARs increased (Joshi et al., 2017). We also found that the GluA1 subunit is critical in sustaining and amplifying status epilepticus (Adotevi et al., 2020). Here, we explored if the global removal of the GluA1 subunit of AMPARs affects postictal apnea occurrence and seizure-induced death.

We recorded simultaneous EEG, breathing, and heartbeat during repeated seizures in GluA1 subunit global knockout (K.O.) mice and their wild-type (W.T.) littermates (Fig. 4A,B). With repeated seizures, GluA1 K.O. mice did not develop postictal apnea compared to W.T. littermates (Fig. 4C). None of the GluA1 K.O. mice developed postictal apnea with recovery (n = 14 mice), whereas 46% of W.T. mice experienced recovery from postictal apnea that lasted 19.63 ± 4.27 s (n = 13 mice). Seizure duration in GluA1 K.O. mice remained unchanged, but in W.T. mice, seizures gradually became longer (GluA1 K.O.: 1^{st} seizure: 17.23 ± 1.14, 10^{th} seizure: 16.85 ± 1.35 s; W.T.: 1^{st} seizure: 17.64 ± 1.03, 10^{th} seizure: 21.45 ± 1.30 s; unpaired t-test, $p < 0.05$, Fig. 4D). Seizure behavior remained the same in GluA1 K.O. mice, but it progressively worsened in W.T.s (Fig. 4E). Only 7% of GluA1 K.O.s had stage 6 seizure compared to 77% of W.T. mice (n = 16 and 18 mice, Fig. 4F). Overall, 93% of GluA1 K.O.s survived compared to only 56% of W.T. littermates at the end of 10^{th} GTCS ($p = 0.012$, Fig. 4G). Deletion of GluA1 subunit of AMPA receptors did not prevent seizures from occurring, but the removal of this subunit alone was sufficient to decrease the probability of death. Thus, repeated seizures gradually enhance GluA1 AMPA receptor-mediated plasticity, increasing the likelihood of postictal apnea and seizure-induced death.

Hippocampal kindling model confirmed: mice without the GluA1 subunit of AMPA receptors cannot sustain repeated GTCSs

Patients with temporal lobe epilepsy (TLE) represent 60% of all epilepsies (Derera et al., 2017). We next confirmed our findings in a second most used model of TLE. Hippocampal kindling is a widely used model and demonstrates that seizures progressively worsen with repetition (Bertram, 2007). We tested if the AMPAR GluA1 subunit was essential for sustaining kindling-induced GTCSs. We implanted bipolar hippocampal electrodes in the ventral CA1 in GluA1 K.O. (n = 10) and their W.T. littermates (n = 10) and kindled them in a pairwise, blinded fashion using traditional kindling methods(Lothman and Williamson, 1992). All animals received 40 stimuli, and then investigators were unblinded.

Both groups kindled at a similar pace initially, exhibiting Racine scale grade 2–3 seizures after the first 25 stimuli. After this, the two groups diverged. W.T. animals progressed to sustained convulsive generalized tonic-clonic seizures (Stages 4&5, Fig. 5A). In contrast, K.O. animals neither attained nor sustained GTCSs. Most GluA1 K.O. mice continued to exhibit grade 2–3 behavioral seizures, and those that exhibited grade 4 or 5 seizures often reverted to a grade 2 or 1 (green arrows), despite repeated stimulation (Fig. 5A). All W.T. mice were kindled, while 60% of GluA1 K.O.s remained unkindled despite stimulation (Fisher's exact test, $p = 0.011$, Fig. 5B). Seizure threshold was higher for K.O. than W.T. animals (GluA1 K.O.: 157.10 ± 37.65 μA; W.T.: 64.00 ± 14.70 μA, Mann Whitney test, $p = 0.022$, Fig. 5C). Seizure severity (median behavioral scores) was lower for all kindled seizures in K.O. animals than in W.T. animals ($p < 0.05$, Mann-Whitney test, Fig. 5D). Seizure duration (after-discharge duration) for the last 5 kindling stimuli was shorter in K.O. animals than in W.T.s (Fig. 5E). Furthermore, two W.T. animals died following GTCS, while none of the K.O. animals died (Fig. 5A). These findings demonstrate that the GluA1 subunit plays a critical role in sustaining repeated generalized tonic-clonic seizures, and increased GluA1 plasticity in W.T. mice contributes to seizure worsening and death.

Drug targeting Ca^{2+}-permeable AMPA receptors prevents apnea and seizure-induced death

AMPA receptors are tetramers, consisting of four subunits GluA1–4 that are assembled as dimers of dimers (Ge and Wang, 2021). AMPA GluA1/GluA2 heteromers play an important role in functional plasticity (Tzakis and Holahan, 2020). GluA1 homomer AMPARs also exist and mediate diverse types of synaptic plasticity (Ge and Wang, 2021). GluA1 subunit is critical for the expression of early LTP, during which GluA1-containing AMPA are recruited into synapses through exocytosis (Ge and Wang, 2021). AMPARs containing GluA2 subunits are calcium-impermeable, but when the proportion shifts in favor of the GluA1 subunit, AMPA receptor properties change, and AMPA receptors become calcium-permeable (Twomey et al., 2018; Wollmuth, 2018) (Fig. 6A). Because global deletion of the GluA1 subunit might have compensatory changes in other subunits in the K.O. mice, we tested whether a drug that pharmacologically inhibits calcium-permeable AMPA receptors would also prevent postictal apnea and mortality. To block Ca^{2+}-permeable AMPA receptors, we used the IEM-1460 drug (Twomey et al., 2018) (Fig. 6A).

We first compared how IEM inhibits Ca^{2+}-permeable AMPA receptor-mediated currents (sEPSCs) in activated versus non-active neurons. We used patch-clamp electrophysiology in c-Fos GFP mice within 20–30 min after a seizure and recorded 10 min baseline followed by 10 min IEM wash (100 μM) in 11 neurons from 6 animals. IEM decreased sEPSCs frequency (KS test, $p < 0.0001$, Fig. 6B) and decreased sEPSCs amplitude (KS test, $p < 0.0001$, Fig. 6C) only in the activated neurons, while IEM did not affect currents in the non-active (untagged) neurons (Fig. 6E,F). This finding indicates that the activated neurons have decreased functional contribution of GluA2-containing AMPA receptors, and GluA2-lacking AMPARs mediate the currents of activated neurons.

We next injected IEM intraperitoneally to determine its effect of blocking Ca^{2+}-permeable AMPA receptors only in activated neurons *in vivo*. IEM (30 mg/kg in saline, i.p., n = 8 mice) or saline (n = 6 mice) were injected in C57BL/6 mice every time 15 min before each repeated seizure (Fig. 6D). None of the IEM-1460 treated mice developed apnea, whereas 5 out of 6 saline-injected mice had postictal apnea and died (Fig. 6G). Similarly, none of the IEM treated mice had stage 6 seizures, while 100% of saline-injected mice had at least one stage 6 seizure (Fig. 6H). Mice treated with IEM had on average shorter seizures compared to saline-injected mice (IEM: 16.56 ± 1.03 s; saline: 20.82 ± 0.66 s. Fig. 6I). 85.7% of all IEM-treated mice survived by the 10^{th} GTCSs compared to 16.7% survival of saline-injected mice (Fig. 6J).

Discussion

We propose that increased excitatory transmission plasticity mediated by AMPA receptors, specifically through the GluA1 subunit, contributes to apnea and seizure-induced death. This death was prevented by IEM-1460, which targets Ca^{2+}-permeable AMPA receptors. Thus, we propose a novel approach to preventing seizure-related apnea and death.

Experiencing generalized tonic-clonic seizures (GTCSs) during the preceding year increased the SUDEP risk 27-fold, whereas no such risk was found in patients with exclusively non-GTCS seizures (Sveinsson et al., 2020). SUDEP risk is 1.2/1,000 patients per year

in children and adults (Ryvlin et al., 2019). In the United States, 3.4 million people have epilepsy, so around 3,000 deaths occur each year due to SUDEP according to the CDC. In resource-limited countries, the mortality is much higher due to a higher number of patients with poorly controlled, refractory seizures. SUDEP is the second leading neurologic cause of potential life-years lost after stroke (Thurman et al., 2014), but despite many available treatments, one-third of patients continue to have seizures (Dworetzky and Kapur, 2017). The current approach to SUDEP prevention includes trying to achieve better GTC seizure control, sharing a bedroom to prevent sleeping alone, adhering to an antiepileptic drug (AED) regimen, and surgery/neuromodulation to achieve seizure freedom (Sveinsson et al., 2020).

Repeated seizures cause progressive behavioral worsening, known as the kindling phenomenon (Bertram, 2007; Lothman et al., 1985; Lothman and Williamson, 1992), and increase the probability of postictal apnea and seizure-induced death (Hesdorffer et al., 2011; Ryvlin et al., 2013; Vilella et al., 2019). In animal studies, the kindling process is traditionally considered complete after three GTCSs. Continuing repeated GTCSs can lead to apnea development similar to human data, indicating apnea is a novel form of kindling-like plasticity.

We find altered brainstem activation alters with seizure repetition. Cortical plasticity and cortical network expansion have been described and associated with kindled seizures and learning and memory (Dabrowska et al., 2019; Kleim et al., 2004; Naik et al., 2022; Taubert et al., 2010; Teskey et al., 2002). Although seizure invasion of the brainstem is well known (Faingold, 2012; Lam et al., 2010; Wengert et al., 2021; Zhang et al., 2018), whether repeated seizures cause brainstem neuronal activation changes and lead to brainstem plasticity has not been described. Enhanced c-Fos expression in the brainstem nuclei is indicative of increased neuronal activation with seizure repetition, but it could also indicate enhanced interneuronal activation in response to increased excitability or altered neuronal firing in response to hypoxia/hypercapnia Furthermore, our studies do not localize the site of plasticity that leads to apnea. Previous studies indicate repeated seizures increase glutamate-dependent, action potential firing rate of GABAergic neurons in the nucleus tractus solitarius of the brainstem (Derera et al., 2017). Here, we used 3D reconstruction mapping to demonstrate that repeated GTCSs cause neuronal activation changes and expand the brainstem seizure network on the cellular level, for example, in such respiratory nuclei as periaqueductal gray (PAG) and dorsal raphe, indicating brainstem activity changes develop with seizure repetition. Optogenetic activation of dorsal raphe serotonin neurons suppresses seizure-induced respiratory arrest, and this effect is reversed by 5-HT_3 receptor antagonist (Zhang et al., 2018). Serotonin neurons in the medullary raphe (i.e., magnus, obscuris, pallidus) also modulate breathing (Corcoran et al., 2009). Because seizures invade respiratory networks (Rhone et al., 2020; Vilella et al., 2019; Wengert et al., 2021; Zhang et al., 2018), and respiratory control is complex (Smith et al., 2013), precise anatomic localization of this seizure-induced plasticity is the focus of our current studies.

AMPA receptors mediate excitatory transmission in the central nervous system, and modulation of their subunit composition plays a role in learning and memory. Although GluA1 subunit K.O. mice have impaired short-term working memory (that requires variation

from trial to trial), these mice retain long-term spatial reference memory (Reisel et al., 2002; Sanderson et al., 2008). Thus, different “types of memories” require different molecular pathways. For example, we have previously demonstrated that mice with globally removed GluA1 subunit cannot learn GluA1-depended memory task, show poor recruitment of memory ensembles, and have no increase in neuronal activation despite repeated learning (Naik et al., 2022). We suggest that seizure “memory” is GluA1 subunit-dependent, and seizure repetition leads to enhanced GluA1 expression. Deleting this subunit alone is sufficient to decrease the probability of postictal apnea and death resulting from repeated seizures, which we confirmed in two separate seizure models. Our pharmacologic inhibition of GluA1 subunit-containing AMPARs indicates that it is a druggable target. We show that inhibiting GluA1-containg AMPA receptors only in the activated neurons, which constitute only a small subset of the total neuronal population, was sufficient to prevent postictal apnea and increase survival of mice fivefold.

Our data support that repeated GTC seizures traffic the GluA1 subunit-containing AMPA receptors to synapses, creating a phenomenon similar to long-term potentiation (LTP), and blocking this mechanism decreases the probability of postictal apnea and seizure-induced death. Although removal/blockade of the GluA1 subunit does not stop seizures from occurring, its removal was sufficient to block seizure-dependent plasticity that leads to death. This elucidates the precise molecular mechanism that contributes to seizure-induced death. The antiepileptic drug Perampanel (Fycompa®) is already an existing, FDA-approved drug that blocks whole AMPA receptors to control focal and generalized seizures. We demonstrate that the specific removal of the GluA1 subunit or targeting Ca^{2+}-permeable AMPA receptors is a potential drug target that could be used as an adjunct therapy for preventing postictal apnea and death. In summary, we identify the GluA1-containg AMPA receptor as a novel therapeutic target for treating patients with drug-refractory GTCSs.

Methods

Animals

The University of Virginia Care and Use Committee approved all experiments. Adult male and female mice (6–12 weeks) were used. 4 mice per cage had ad libitum food and water access and were maintained on a 12 hr light / 12 hr dark cycle. For genotyping, the KAPA Biosystems kit was used. C57BL/6 mice were obtained from Charles River. To generate TRAP2 mice, mice expressing Cre-ER under the regulation of the c-Fos promoter ($Fos^{2A\text{-}ICreERT2}$, Jackson Laboratories, #030323) were crossed to mice expressing tdTomato from the Rosa locus (Ai9, Jackson Laboratories, #007909). We have previously injected homecage TRAP2 mice with saline instead of PTZ to exclude leaky expression (Naik et al., 2021). For electrophysiological recordings, TetTag mice (c-Fos-GFP mice) were generated by crossing Tg strain mice ((tetO-HIST1H2BJ/GFP) 46Efu/J, #005104) to mice that express tetracycline-transactivator (tTA) protein under c-Fos promoter (fos-tTA, gifted by B. Wiltgen)(Naik et al., 2021; Reijmers et al., 2007). cFos-GFP mice were born and raised on doxycycline-containing chow (40 mg/kg) to prevent GFP expression prior to the experiments(Reijmers et al., 2007). The GluR1 global knockouts (K.O.s) were obtained from Seeburg (Max-Plank Institute for Medical Research, Heidelberg, Germany) and have

been characterized in detail previously (Adotevi et al., 2020; Mack et al., 2001; Zamanillo et al., 1999). Their wild-type (W.T.) littermates were controls.

Seizure induction

A week after EEG/ECG surgery, mice received a single PTZ injection (50 mg/kg, i.p., Sigma Cat. # P6500) in the plethysmography chamber every other day for a total of 10 injections. To describe seizure intensity, we used the following Racine scale: stage 1 – mouth/facial movements, stage 2 – head nodding, stage 3 – unilateral forelimb clonus, stage 4 – bilateral forelimb clonus with rearing, stage 5 – rearing and falling, stage 6 – involuntary jumping/ wild running. None of the mice had status epilepticus (seizures longer than 5 min) or seizure clusters; all mice had only single discrete generalized tonic-clonic seizures.

For electrophysiological recordings, cFos-GFP mice (4–6 weeks) were removed from doxycycline chow 48 hrs before receiving a single PTZ injection and were observed for a seizure. Mice were processed for electrophysiological recordings within 20–30 min after a seizure as described below.

For kindling, mice were stereotaxically implanted with a stimulating bipolar electrode made of two twisted insulated stainless-steel wires in the left ventral CA1 hippocampus, bilateral cortical electrodes, and a cerebellar reference. The animals were connected to a video-EEG monitoring system after a week recovery. An after-discharge threshold (ADT) was determined for each animal by applying a 1 ms biphasic squared wave pulse at 50 Hz for 1 s to the bipolar hippocampal electrode. Initial stimulation with a pulse amplitude of 20 μA was applied, followed by successive stimulations of 20 μA increases applied at 2 min intervals, until a seizure of at least 10 s was observed for both cortical electrodes on the EEG. Afterwards, electrical stimulation was performed daily with a pulse amplitude of 125% ADT.

EEG/ECG/breathing recordings

Mice were anesthetized with isoflurane and surgically implanted with a headset with two subdural bilateral EEG electrodes in the frontal lobe and a cerebellar reference. ECG leads connected to the same headset were fed through the tubing under the skin to contact the left diaphragm and right shoulder reference and sutured in place as shown in this video publication (Mishra et al., 2018). ECG signal was amplified at 2000 and bandpass filtered between 30–300 Hz with an analog amplifier (Neurodata Model 12, Grass Instruments Co.).

Mice were individually housed in plethysmography chambers custom-designed by Dr. Ian Wenker with Rhino 7 software (Wengert et al., 2021). The Plexiglas was laser-cut with floor dimensions of 4.5 × 4.5 inches (> 20 sq. inches) and 7 inches tall with ports for air in and out and for pressure monitoring. The chambers were supplied with a continuous flow of room air at 400 ml/min via supply and exhaust air pumps (MK-1504 Aquarium Air Pump, AQUA Culture) balanced to maintain chamber pressure near atmospheric. The surgically implanted EEG headsets were connected to a swivel cable, allowing mice to move freely in the chamber. Mice were placed and video monitored for 30 min to record breathing baseline. After, they were given a single PTZ injection and left for another 30 min recording after a seizure.

To assess breathing frequency, the pressure changes between the animal and reference chambers were measured with an analog pressure transducer (SDP1000-L05, Sensirion). The signals were digitized with a Powerlab 16/35 digitizer and recorded with LabChart 7 software (AD Instruments, Inc.) at 1 kHz/s. Video recorded by multiplexing miniature night vision-enabled cameras was digitized with a Dazzle Video Capture Device (Corel, Inc.) and recorded at 30 fps with LabChart 7 in tandem with biosignals. The apnea region was defined at least half of the baseline amplitude breathing recording, resembling a trace without a mouse in the chamber, with an interbreath interval that is > 1 s.

Immunohistochemistry, confocal imaging, and 3D brain reconstruction

Mice were deeply anesthetized with isoflurane and perfused intracardially with 4% paraformaldehyde (PFA) in 0.1 M PB, pH 7.2 at 4°C. Brains were fixed in PFA overnight, cryoprotected in 30% sucrose in PBS for 2 days at 4°C and sliced on a cryostat at 45 μm. Sections for staining were placed in a blocking buffer (50 ml/ml normal goat serum (NGS), #017-000-121, Jackson ImmunoResearch, and 0.1% TritonTM X-100) for 2 h. The primary antibodies (with 20 ml/ml NGS overnight at 4°C) were rabbit anti-ARC (1:1000, 156003, Synaptic Systems) and rabbit anti-c-Fos (1:1000, ab190289, Abcam). The secondary antibody was 488 goat anti-rabbit (1:500, Invitrogen, for 2 h at room temp.). Confocal images were done on Nikon Eclipse Ti-U at 10x/0.45 NA, 20x/0.95 NA (for ARC), 1024 × 1024 frame size. Images were tiled as stacks at 5 μm z-interval and stitched using NIS-Elements software. Imaris 9.9.1 (Bitplane) was used for visualization. ImageJ was used to colocalize tdTomato positive neurons (first seizure) and c-Fos labeled neurons (second seizure). Adobe Photoshop Elements and BioRender were used for figure display. For 3D brain reconstruction, every serial section was collected, DAPI stained, imaged, and stacked in the NeuroInfo software (MBF Bioscience). To identify brain regions, sections were mapped onto the digital Allen Mouse Brain Atlas in the software, and cells were counted in the regions of interest.

Patch-clamp electrophysiology

All chemicals were obtained from Sigma or Fisher Scientific unless otherwise stated. 20–30 min following a single PTZ seizure (50 mg/kg, i.p.), cFos-GFP mice were deeply anesthetized with isoflurane, and brains were quickly removed and immersed in oxygenated (95% O_2/5% CO_2) ice-cold (0–4 °C) slicing buffer (in mM, 65.5 NaCl, 2 KCl, 5 $MgSO_4$, 25 $NaHCO_3$, 1.1 KH_2PO_4, 1 $CaCl_2$, 10 glucose, and 113 sucrose; 300 mOsm, pH 7.35 to 7.45). To obtain the optimal motor cortex region (M1 and M2), coronal slices from the frontal lobe (300 −350 μm thick) were prepared by an oblique cut (approximately 60°) using a vibratome (VT1200S, Leica). The slices were then transferred to an incubation chamber at 33 °C in artificial cerebrospinal fluid (aCSF, containing in mM, 127 NaCl, 2 KCl, 1.5 $MgSO_4$, 25.7 $NaHCO_3$, 10 glucose, and 1.5 $CaCl_2$; 300 mOsm, bubbled with 95% O_2/5% CO_2, pH 7.35 to 7.45).

Motor cortex (primary and secondary) layer 2/3 pyramidal neurons activated by seizures were identified based on GFP fluorescence using Nikon Eclipse FN1 with a fluorescent source. Tagged and untagged neurons were studied in random order. During the recording, slices were transferred to a recording chamber perfused with aCSF at 2–3 ml/min.

Recordings were performed using a Multiclamp 700A amplifier (Molecular Devices). The data were collected using pClamp 10.2 software (Molecular Devices), filtered at 2 kHz, and sampled at 10 kHz (Digidata 1440A, Molecular Devices). Recording pipettes were fabricated from borosilicate glass (1.5 mm outer diameter, 0.86 mm inner diameter, Sutter Instrument) using a Flaming-Brown micropipette puller (P-1000, Sutter Instruments). Resting membrane potential was recorded in zero current-clamp mode just after the electrode broke in the cells. Only membrane potential below - 55 mV was acceptable for data collection. Membrane time constants were experimentally determined as the time for the potential fell from the resting to a fraction (1-I/e), or 63%, of its final value in the charging curve during the application of a small negative current pulse. Membrane resistance was obtained from membrane potentials in response to current injections without action potential (A.P.) evoked. The slope of liner fit of the I-V curve was calculated as membrane resistance. A.P. was evoked by the current injection. A.P. was evoked during current injections, and the initial point of the A.P. upstroke phase was the threshold. A.P. amplitude was the height between the A.P. peak and its afterhyperpolarization (AHP) for the first A.P. evoked. A.P. wide was the time between the upstroke phase and repolarizing phase at 50% of A.P. amplitude. Current injections were performed from −100 pA to 300 pA with 20 pA increasing steps and lasted for 500 ms. To compare firing patterns between neurons, membrane potential was adjusted to −65 mV by using a small amount of current before the injections.

EPSCs recordings were in voltage-clamp mode. Tight-seal whole-cell recordings were obtained using standard techniques. Recording pipettes had open-tip resistances of 6–8 MΩ and were filled with the internal solution (in mM, 110 D-gluconic acid, 110 CsOH, 10 CsCl, 1 EGTA, 1 $CaCl_2$, 10 HEPES, 5 Mg-ATP, and 5 lidocaine; 290 mOsm, pH 7.3). Electrode capacitance was electronically compensated. Access resistance was continuously monitored, and if the series resistance increased by 20% at any time, the recording was terminated. Layer 2/3 cells were identified visually, patched in voltage-clamp configuration and recorded in a holding potential of −65 mV for EPSCs. Current-clamp recordings were performed in tight-seal (seal ≥ 1 GΩ) for the measurement of cell membrane properties and for biocytin filling into the cell. Internal solution was (in mM): 135 K-gluconate, 7 KCl, 10 HEPES, 0.5 EGTA, 2.5 NaCl, 4 Mg-ATP, and 0.3 Na-GTP. For biocytin labeling, 5% biocytin was added to the internal solution, and recording was continued for 20–50 min. Amplitude, frequency of sEPSCs, and decay kinetics were evaluated using weighted tau. Current-clamp data was analyzed using Clampex 10.5 and MiniAnalysis.

IEM-1460 drug treatment

To block calcium-permeable (GluA2-lacking) AMPA receptors, we used IEM-1460 (Tocris Bioscience, Cat. #1636, *N,N,H,*-Trimethyl-5-[(tricyclo[3.3.1.13,7]dec-1-ylmethyl)amino]-1-pentanaminiumbromide hydrobromide). For patch-clamp electrophysiology, we recorded a 10 min baseline in motor cortical slices of c-Fos GFP mice within 20–30 min after a seizure followed by continuous 10 min IEM-1460 wash (100 μM) and recording after, while still washing with IEM. Recordings from the control nonactive (untagged) cells were done on separate slices because IEM wash prevented recording a second time from the same slice.

For the i.p. injections, either IEM-1460 (30 mg/kg in saline) or saline was used 15 min before each PTZ repeated seizure.

Statistics

We analyzed data using Prism 9.5.0 and presented them as mean ± SEM, where n is the number of animals. Results were considered statistically significant for $p < 0.05$, where *$p < 0.05$, **$p < 0.01$, ***$p < 0.001$, ****$p < 0.0001$. All data were tested for normality. Two groups were compared with either paired t-test (for cell recordings in the same slice), unpaired t-test, or the Kolmogorov-Smirnov test. Multiple groups were compared with one-way ANOVA with multiple comparisons. Because the sEPSC amplitudes and frequency are often not normally distributed, we used cumulative probability instead of means.

Acknowledgments

This work was supported by the National Institutes of Health (RO1 NS040337, RO1 NS044370 to J.K.) and the UVA Brain Institute. Laser cutting for the plethysmography chambers was performed at the Fab lab, Department of Architecture, University of Virginia. We also thank the rest of the Kapur lab for valuable comments on this study.

Data availability

The data that support the findings are available from the corresponding authors upon request.

References

Adotevi N, Lewczuk E, Sun H, Joshi S, Dabrowska N, Shan S, Williamson J, Kapur J, 2020. α-Amino-3-hydroxy-5-methyl-4-isoxazolepropionic acid receptor plasticity sustains severe, fatal status epilepticus. Ann. Neurol 87, 84–96. [PubMed: 31675128]

Allen WE, DeNardo LA, Chen MZ, Liu CD, Loh KM, Fenno LE, Ramakrishnan C, Deisseroth K, Luo L, 2017. Thirst-associated preoptic neurons encode an aversive motivational drive. Science 357, 1149–1155. [PubMed: 28912243]

Bertram E, 2007. The relevance of kindling for human epilepsy. Epilepsia 48, 65–74.

Corcoran A, Hodges M, Wu Y, Wang W, Wylie C, Deneris E, Richerson G, 2009. Medullary serotonin neurons and central CO2 chemoreception. Respir Physiol Neurobiol 168, 49–58. [PubMed: 19394450]

Dabrowska N, Joshi S, Williamson J, Lewczuk E, Lu Y, Oberoi S, Brodovskaya A, Kapur J, 2019. Parallel pathways of seizure generalization. Brain 142, 2336–2351. [PubMed: 31237945]

Derera ID, Delisle BP, Smith BN, 2017. Functional neuroplasticity in the nucleus tractus solitarius and increased risk of sudden death in mice with acquired temporal lobe epilepsy. eNeuro 4.

Devinsky O, Hesdorffer DC, Thurman DJ, Lhatoo S, Richerson G, 2016. Sudden unexpected death in epilepsy: epidemiology, mechanisms, and prevention. Lancet Neurol. 15, 1075–1088. [PubMed: 27571159]

Dworetzky BA, Kapur J, 2017. Gaining perspective on SUDEP: The new guideline. Neurology 88, 1598–1599. [PubMed: 28438840]

Faingold CL, 2012. Brainstem networks reticulo-cortical synchronization in generalized convulsive seizures, in: Noebels J, Avoli M, Rogawski M, Olsen R, Delgado-Escueta A (Eds.), Jasper's Basic Mechanisms of the Epilepsies. Bethesda, pp. 257–271.

Fortin DA, Davare MA, Srivastava T, Brady JD, Nygaard S, Derkach VA, Soderling TR, 2010. Long-term potentiation-dependent spine enlargement requires synaptic Ca2+-permeable AMPA receptors recruited by CaM-kinase I. J. Neurosci 30, 11565–11575. [PubMed: 20810878]

Ge Y, Wang YT, 2021. GluA1-homomeric AMPA receptor in synaptic plasticity and neurological diseases. Neuropharmacology 197, 108708. [PubMed: 34274350]

Guenthner CJ, Miyamichi K, Yang HH, Heller HC, Luo L, 2013. Permanent genetic access to transiently active neurons via TRAP: Targeted recombination in active populations. Neuron 79, 773–784.

Harden C, Tomson T, Gloss D, Buchhalter J, Cross JH, Donner E, French JA, Gil-Nagel A, Hesdorffer DC, Smithson WH, Spitz MC, Walczak TS, Sander JW, Ryvlin P, 2017. Practice guideline summary: sudden unexpected death in epilepsy incidence rates and risk factors. Neurology 88, 1674–1680. [PubMed: 28438841]

Hesdorffer DC, Tomson T, Benn E, Sander JW, Nilsson L, Langan Y, Walczak TS, Beghi E, Brodie MJ, Hauser A, 2011. Combined analysis of risk factors for SUDEP. Epilepsia 52, 1150–1159. [PubMed: 21671925]

Hughlings Jackson J, 1890. The Lumleian Lectures on convulsive seizures. Lancet 135, 785–788.

Joshi S, Rajasekaran K, Sun H, Williamson J, Kapur J, 2017. Enhanced AMPA receptor-mediated neurotransmission on CA1 pyramidal neurons during status epilepticus. Neurobiol. Dis 103.

Kim Y, Bravo E, Thirnbeck CK, Smith-Mellecker LA, Kim SH, Gehlbach BK, Laux LC, Zhou X, Nordli DR, Richerson GB, 2018. Severe peri-ictal respiratory dysfunction is common in Dravet syndrome. J. Clin. Investig 128, 1141–1153. [PubMed: 29329111]

Kleim JA, Hogg TM, VandenBerg PM, Cooper NR, Bruneau R, Remple M, 2004. Cortical synaptogenesis and motor map reorganization occur during late, but not early, phase of motor skill learning. J. Neurosci 24, 628–633. [PubMed: 14736848]

Kommajosyula SP, Randall ME, Brozoski TJ, Odintsov BM, Faingold CL, 2017. Specific subcortical structures are activated during seizure-induced death in a model of sudden unexpected death in epilepsy (SUDEP): A manganese-enhanced magnetic resonance imaging study. Epilepsy Res. 135, 87–94. [PubMed: 28646692]

Lam A, Whelan N, Corcoran ME, 2010. Susceptibility of brainstem to kindling and transfer to the forebrain. Epilepsia 51, 1736–1744. [PubMed: 20384715]

Lewczuk E, Joshi S, Williamson J, Penmetsa M, Shan S, Kapur J, 2018. Electroencephalography and behavior patterns during experimental status epilepticus. Epilepsia 59, 369–380. [PubMed: 29214651]

Lothman EW, Hatlelid JM, Zorumski CF, Conry JA, Moon PF, Perlin JB, 1985. Kindling with rapidly recurring hippocampal seizures. Brain Res. 360, 83–91. [PubMed: 3000538]

Lothman EW, Williamson JM, 1992. Influence of electrical stimulus parameters on after discharge thresholds in the rat hippocampus. Epilepsy Res. 13, 205–213. [PubMed: 1493783]

Mack V, Burnashev N, Kaiser KMM, Rozov A, Jansen V, Hvalby Ø, Seeburg PH, Sakmann B, Sprengel R, 2001. Conditional restoration of hippocampal synaptic potentiation in GluR-A-deficient mice. Science (80-.). 292, 2501–2504.

Malinow R, 2003. AMPA receptor trafficking and long-term potentiation. Philos. Trans. R. Soc. B Biol. Sci 358, 707–714.

Massey CA, Sowers LP, Dlouhy BJ, Richerson GB, 2014. Mechanisms of sudden unexpected death in epilepsy: The pathway to prevention. Nat. Rev. Neurol 10, 271–282. [PubMed: 24752120]

Mishra V, Gautier NM, Glasscock E, 2018. Simultaneous video-EEG-ECG monitoring to identify neurocardiac dysfunction in mouse models of epilepsy. J. Vis. Exp 131.

Miyamoto D, Marshall W, Tononi G, Cirelli C, 2021. Net decrease in spine-surface GluA1-containing AMPA receptors after post-learning sleep in the adult mouse cortex. Nat. Commun 12.

Naik AA, Brodovskaya A, Subedi S, Akram A, Kapur J, 2022. Extrahippocampal seizure and memory circuits overlap. eNeuro 9.

Naik AA, Sun H, Williams CL, Weller DS, Julius Zhu J, Kapur J, 2021. Mechanism of seizure-induced retrograde amnesia. Prog. Neurobiol 200.

Nashef L, 1997. Sudden unexpected death in epilepsy: terminology and definitions. Epilepsia 38, S6–S8.

Nashef L, So EL, Ryvlin P, Tomson T, 2012. Unifying the definitions of sudden unexpected death in epilepsy. Epilepsia 53, 227–233. [PubMed: 22191982]

Patodia S, Somani A, O'Hare M, Venkateswaran R, Liu J, Michalak Z, Ellis M, Scheffer IE, Diehl B, Sisodiya SM, Thom M, 2018. The ventrolateral medulla and medullary raphe in sudden unexpected death in epilepsy. Brain 141, 1719–1733. [PubMed: 29608654]

Patterson MA, Szatmari EM, Yasuda R, 2010. AMPA receptors are exocytosed in stimulated spines and adjacent dendrites in a Ras-ERK-dependent manner during long-term potentiation. Proc. Natl. Acad. Sci. U. S. A 107, 15951–15956. [PubMed: 20733080]

Penfield W, Jasper HH, 1954. Epilepsy and the functional anatomy of the human brain. Little, Brown, Boston.

Petrucci AN, Joyal KG, Purnell BS, Buchanan GF, 2020. Serotonin and sudden unexpected death in epilepsy. Exp. Neurol 325.

Rajasekaran K, Joshi S, Sun C, Mtchedlishvilli Z, Kapur J, 2010. Receptors with low affinity for neurosteroids and GABA contribute to tonic inhibition of granule cells in epileptic animals. Neurobiol. Dis 40.

Rajasekaran K, Todorovic M, Kapur J, 2012. Calcium-permeable AMPA receptors are expressed in a rodent model of status epilepticus. Ann. Neurol 72.

Rakhade SN, Zhou C, Aujla PK, Fishman R, Sucher NJ, Jensen FE, 2008. Early alterations of AMPA receptors mediate synaptic potentiation induced by neonatal seizures. J. Neurosci 28, 7979–7990. [PubMed: 18685023]

Reijmers LG, Perkins BL, Matsuo N, Mayford M, 2007. Localization of a stable neural correlate of associative memory. Science (80-.). 317, 1230–1233.

Reisel D, Bannerman DM, Schmitt WB, Deacon RMJ, Flint J, Borchardt T, Seeburg PH, Rawlins JNP, 2002. Spatial memory dissociations in mice lacking GluR1. Nat. Neurosci 5, 868–873. [PubMed: 12195431]

Rhone AE, Kovach CK, Harmata GIS, Sullivan AW, Tranel D, Ciliberto MA, Howard MA, Richerson GB, Steinschneider M, Wemmie JA, Dlouhy BJ, 2020. A human amygdala site that inhibits respiration and elicits apnea in pediatric epilepsy. JCI Insight 5.

Roth RH, Cudmore RH, Tan HL, Hong I, Zhang Y, Huganir RL, 2020. Cortical synaptic AMPA receptor plasticity during motor learning. Neuron 105, 895–908.e5. [PubMed: 31901303]

Ryvlin P, Nashef L, Lhatoo SD, Bateman LM, Bird J, Bleasel A, Boon P, Crespel A, Dworetzky BA, Høgenhaven H, Lerche H, Maillard L, Malter MP, Marchal C, Murthy JMK, Nitsche M, Pataraia E, Rabben T, Rheims S, Sadzot B, Schulze-Bonhage A, Seyal M, So EL, Spitz M, Szucs A, Tan M, Tao JX, Tomson T, 2013. Incidence and mechanisms of cardiorespiratory arrests in epilepsy monitoring units (MORTEMUS): a retrospective study. Lancet Neurol. 12, 966–977. [PubMed: 24012372]

Ryvlin P, Rheims S, Lhatoo SD, 2019. Risks and predictive biomarkers of sudden unexpected death in epilepsy patient. Curr. Opin. Neurol 32, 205–212. [PubMed: 30694923]

Sanderson DJ, Good MA, Seeburg PH, Sprengel R, Rawlins JNP, Bannerman DM, 2008. The role of the GluR-A (GluR1) AMPA receptor subunit in learning and memory. Prog. Brain Res 169, 159–178. [PubMed: 18394473]

Shimshek DR, Bus T, Schupp B, Jensen V, Marx V, Layer LE, Köhr G, Sprengel R, 2017. Different forms of AMPA receptor mediated LTP and their correlation to the spatial working memory formation. Front. Mol. Neurosci 10.

Smith JC, Abdala APL, Borgmann A, Rybak IA, Paton JFR, 2013. Brainstem respiratory networks: building blocks and microcircuits. Trends Neurosci. 36, 152–162. [PubMed: 23254296]

Sveinsson O, Andersson T, Mattsson P, Carlsson S, Tomson T, 2020. Clinical risk factors in SUDEP: a nationwide population-based case-control study. Neurology 94, e419–e429. [PubMed: 31831600]

Taubert M, Draganski B, Anwander A, Müller K, Horstmann A, Villringer A, Ragert P, 2010. Dynamic properties of human brain structure: learning-related changes in cortical areas and associated fiber connections. J. Neurosci 30, 11670–11677. [PubMed: 20810887]

Teran FA, Bravo E, Richerson GB, 2022. Sudden unexpected death in epilepsy: Respiratory mechanisms. Handb. Clin. Neurol 189, 153–176. [PubMed: 36031303]

Teskey C, Monfils M, VanderBerg P, Kleim J, 2002. Motor map expansion following repeated cortical and limbic seizures is related to synaptic potentiation. Cereb. Cortex 12, 98–105. [PubMed: 11734536]

Thurman DJ, Hesdorffer DC, French JA, 2014. Sudden unexpected death in epilepsy: assessing the public health burden. Epilepsia 55, 1479–1485. [PubMed: 24903551]

Tomson T, Nashef L, Ryvlin P, 2008. Sudden unexpected death in epilepsy: current knowledge and future directions. Lancet Neurol. 7, 1021–1031. [PubMed: 18805738]

Twomey EC, Yelshanskaya MV, Vassilevski AA, Sobolevsky AI, 2018. Mechanisms of channel block in calcium-permeable AMPA receptors. Neuron 99, 956–968.e4. [PubMed: 30122377]

Tzakis N, Holahan MR, 2020. Investigation of GluA1 and GluA2 AMPA receptor subtype distribution in the hippocampus and anterior cingulate cortex of Long Evans rats during development. IBRO Reports 8, 91–100. [PubMed: 32300670]

Vilella L, Lacuey N, Hampson JP, Rani MRS, Sainju RK, Friedman D, Nei M, Strohl K, Scott C, Gehlbach BK, Zonjy B, Hupp NJ, Zaremba A, Shafiabadi N, Zhao X, Reick-Mitrisin V, Schuele S, Ogren J, Harper RM, Diehl B, Bateman L, Devinsky O, Richerson GB, Ryvlin P, Lhatoo SD, 2019. Postconvulsive central apnea as a biomarker for sudden unexpected death in epilepsy (SUDEP). Neurology 92, e171–e182. [PubMed: 30568003]

Wengert ER, Wenker IC, Wagner EL, Wagley PK, Gaykema RP, Shin JB, Patel MK, 2021. Adrenergic mechanisms of audiogenic seizure-induced death in a mouse model of SCN8A encephalopathy. Front. Neurosci 15.

Wollmuth LP, 2018. Ion permeation in ionotropic glutamate receptors: still dynamic after all these years. Curr. Opin. Physiol 2, 36–41. [PubMed: 29607422]

Xia M, Owen B, Chiang J, Levitt A, Preisinger K, Yan WW, Huffman R, Nobis WP, 2022. Disruption of synaptic transmission in the bed nucleus of the stria terminalis reduces seizure-induced death in DBA/1 mice and alters brainstem E/I balance. ASN Neuro 14.

Zamanillo D, Sprengel R, Hvalby Ø, Jensen V, Burnashev N, Rozov A, Kaiser KMM, Köster HJ, Borchardt T, Worley P, Lübke J, Frotscher M, Kelly PH, Sommer B, Andersen P, Seeburg PH, Sakmann B, 1999. Importance of AMPA receptors for hippocampal synaptic plasticity but not for spatial learning. Science (80-.). 284, 1805–1811.

Zhang H, Zhao H, Zeng C, Van Dort C, Faingold CL, Taylor NE, Solt K, Feng HJ, 2018. Optogenetic activation of 5-HT neurons in the dorsal raphe suppresses seizure-induced respiratory arrest and produces anticonvulsant effect in the DBA/1 mouse SUDEP model. Neurobiol. Dis 110, 47–58. [PubMed: 29141182]

Highlights

- Repeated generalized seizures are the most significant risk factor for SUDEP
- Repeated mouse seizures led to apnea, death, and larger activated neuronal network
- Activated neurons had enhanced, Ca^{2+} permeable, AMPA receptor-mediated transmission
- Global deletion of the AMPAR GluA1 subunit abolished seizure-induced apnea and death
- Drug blockade of Ca^{2+}-permeable AMPARs reduced apnea and death

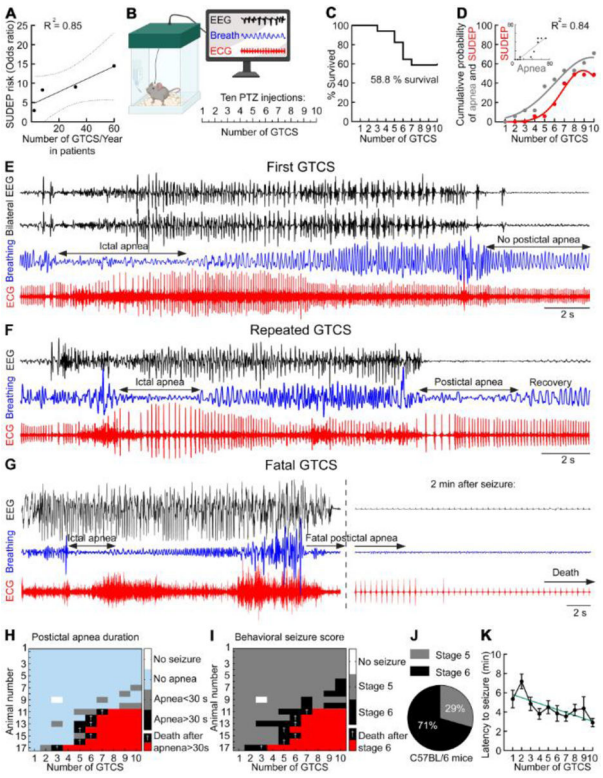

Fig. 1. Repeated generalized seizures gradually worsen, leading to postictal apnea and death.

(A) Human SUDEP risk increases as a function of yearly GTCS frequency (data plotted from Hesdorfer et al. 2011, Epilepsia(Hesdorffer et al., 2011)). (B) We recorded EEG, breathing, and heartbeat simultaneously as mice experienced GTCSs every other day for 10 seizures. (C) Kaplan-Meier survival curve demonstrates decreased survival with repeated seizures. (D) Cumulative probability of postictal apnea and seizure-induced death increase with repeated GTCSs. Inset graph: Apnea correlates with death. (E) Representative bilateral EEG recording (black), breathing (blue), and heartbeat (red) of a first seizure with ictal apnea only. (F) Repeated seizure with postictal apnea and subsequent recovery from it. (G) Fatal repeated GTCS with terminal postictal apnea and gradual bradycardia. (H) Postictal apnea occurred more frequently as the number of GTCSs (columns) increased in individual C57BL/6 mice (rows, n = 17). Grey and black indicate postictal apnea duration (< or > 30 s), and white crosses indicate death day. (I) Behavioral seizures worsened with repeated GTCSs (columns) in individual C57BL/6 mice (rows). Grey and black indicate stage 5 or 6 seizures, and white crosses indicate death day. (J) Ratio of mice that had only stage 5 seizures (grey) vs at least one stage 6 seizure (black). (K) Latency to seizure onset (min) decreased with repetition. Data are mean ± SEM.

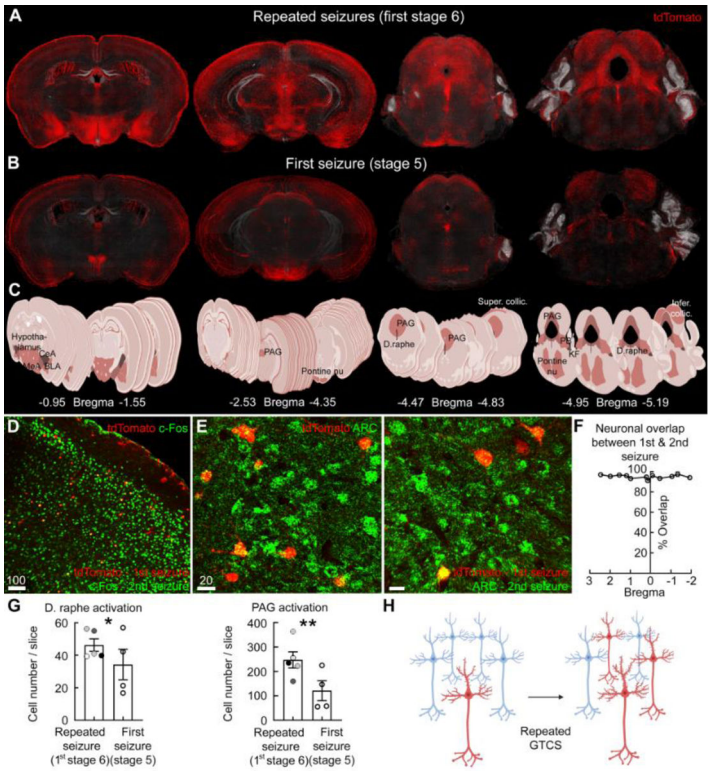

Fig. 2. Seizures repeat and expand network, causing brainstem plasticity.

(A) 3D brain reconstruction with sequential 45 μm sections overlaid on top of each other as shown in c after four repeated GTCSs (the first stage 6 seizure occurred on day 4) vs (B) after a single stage 5 seizure in TRAP2 mice. (C) Schematic of the number and location of slices used for 3D reconstruction in a and b. CeA – central amygdala, MeA – medial amygdala, BLA – basolateral amygdala, PAG – periaqueductal gray, D. raphe – dorsal raphe, P.B. – parabrachial nucleus, K.F. – Kölliker-Fuse nucleus. (D) Repeated second seizure (green, c-Fos, or (E) ARC) recruits the same neurons as the first seizure (red, tdTomato) plus additional neurons, expanding the network. (F) Quantification demonstrates % of neurons active during the first seizure that were also active during the second seizure across the motor cortex. (G) Quantification of the number of cells per slice in the dorsal raphe and PAG nucleus in TRAP2 mice after repeated seizures (n = 5 mice) vs after the first seizure (n = 4 mice). Color gradation of symbols in the first column represents the number of repeated seizures that occurred before quantification (1st stage 6 seizure on: day 1 (white), day 4 (light grey), day 6 (dark grey), day 9 (black)). (H) GTCSs expand the neuronal circuits active during subsequent GTCSs, activating the first initial neurons and additional ones. Data are mean ± SEM, *p < 0.05, **p< 0.01.

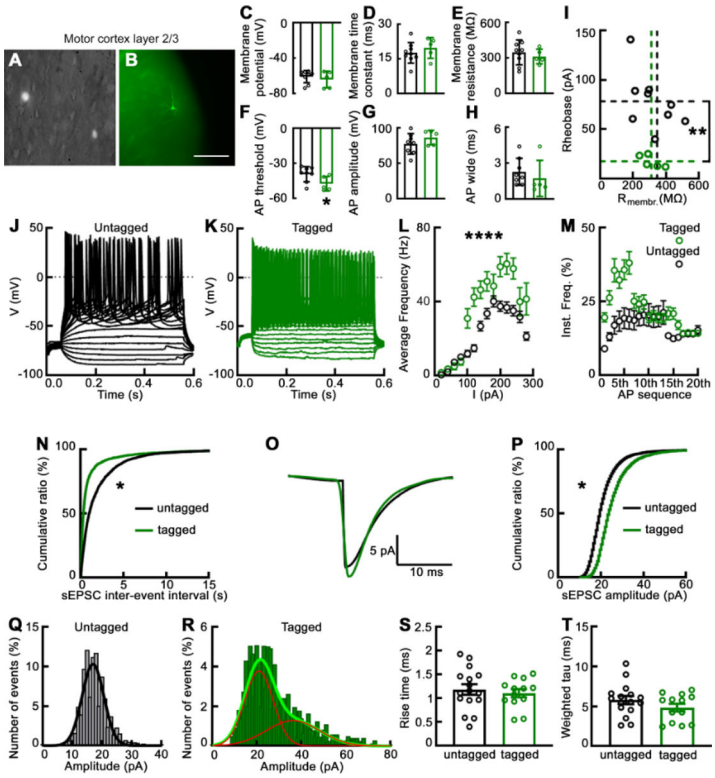

Fig. 3. Seizure-activated neurons are more excitable than nonactive neurons and demonstrate enhanced AMPA transmission after a single seizure.

(A) A fluorescent/DIC image shows bright tagged neurons in layer 2/3 of the motor cortex in an acute brain slice of a TetTag mouse after a single seizure. (B) An example of motor cortical layer 2/3 pyramidal neuron filled with biocytin during the recording. All recorded neurons were identified post-hoc. (c) The rest membrane potentials, (D) membrane time constant, (E) membrane resistance were similar in tagged (green) and untagged (black) neurons. (F) Action potential (A.P.) threshold was lower in tagged (green) than untagged (black) neurons. (G) A.P. amplitudes, (H) A.P. wide were similar in tagged (green) and untagged (black) neurons. (I) Similar membrane resistance but lower rheobase current was in tagged (green) than untagged (black) neurons. Dashed lines show the mean values. (J,K) The representative traces illustrate action potentials evoked at different current injections. (L) Frequency-current (F-I) plot illustrates a higher frequency of action potentials evoked by each current injection in tagged neurons. (M) Instantaneous frequency vs action potential sequence based on analysis of A.P.s evoked by current injection, examples are shown are in j and k. (N) Cumulative ratio (%) of sEPSC inter-event intervals in tagged (green) and untagged neurons (black). (O) Average sEPSC traces from a tagged (green) and an untagged surrounding neuron (black). (P) Cumulative ratio (%) of sEPSC amplitudes in tagged (green) and untagged neurons (black). (Q) The frequency distribution of sEPSCs for 16 untagged neurons fitted with Gaussian distribution (black line). (R) The frequency distribution of sEPSCs for 13 tagged neurons with the sum of two Gaussian distributions (green curve) and two separated single Gaussian distributions (red curves). (S) Rise time was similar in tagged and untagged neurons. (T) Weighted decay tau was similar in tagged and

untagged neurons. Data are mean ± SEM (SD: c-h), n = 11 per group, *p < 0.05, **p< 0.01, ****p< 0.0001.

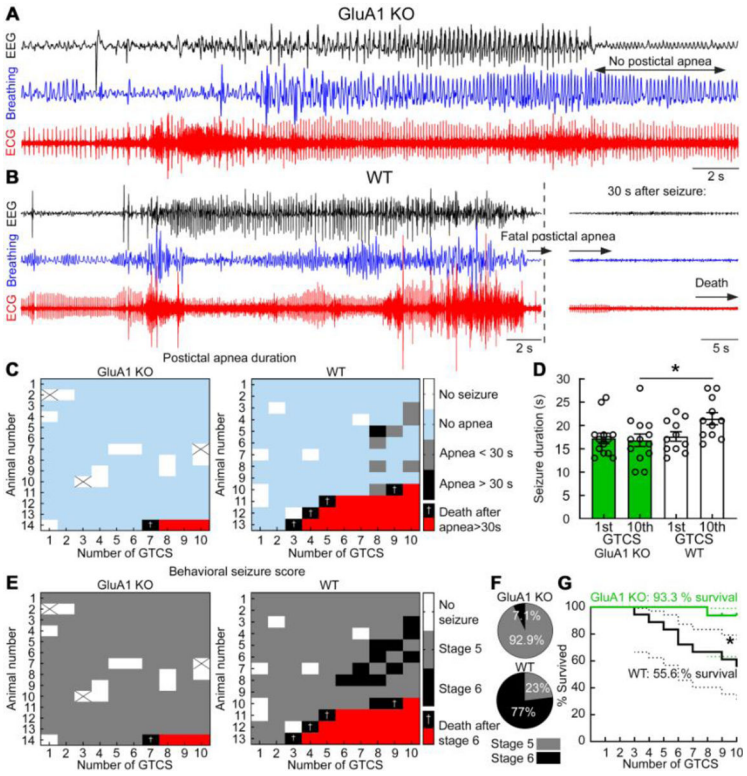

Fig. 4. Mice without the GluA1 subunit of AMPA receptor do not develop postictal apneas, have less severe seizures, and survive.

(A,B) Representative EEG (black), breathing (blue), and heartbeat (red) recordings in a GluA1 K.O. mouse without postictal apnea and a W.T. littermate with fatal postictal apnea and gradual bradycardia until death. (C) Postictal apneas appeared more frequently in W.T. compared to GluA1 K.O. mice with repeated seizures (crossed white background indicates headset fell out or breathing recording not saved). (D) Seizures in W.T. mice became progressively longer compared to K.O. mice, in which they stayed of the same duration (each point represents a single mouse). (E) Seizure behavior became more severe with repetition in W.T. than in GluA1 K.O. mice. (F) W.T. mice had more stage 6 (black) seizures than GluA1 K.O.s. (G) Kaplan-Meyer survival curve demonstrates more GluA1 K.O.s survived than W.T.s. Data are mean ± SEM, *p < 0.05, ****p< 0.0001.

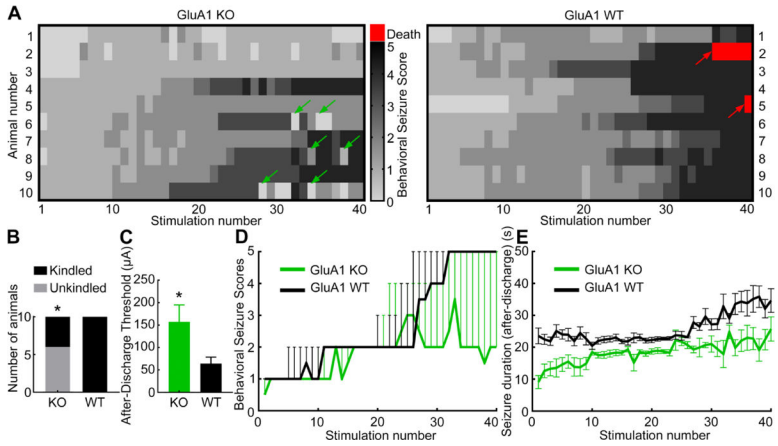

Fig. 5. GluA1 subunit of AMPA receptors sustains repeated GTCSs.

(A) Heat maps illustrate the severity of behavioral seizure scores in GluA1 K.O. vs W.T. mice (red indicates death; black indicates more severe seizures; rows signify individual animals (10 animals were randomly chosen to represent each group)). (B) All W.T. mice were kindled, whereas 60% of GluA1 K.O. mice remained unkindled despite stimulation. (C) Threshold to induce seizure was higher in GluA1 K.O. than in W.T. mice. (D) Behavioral seizure scores were lower in GluA1 K.O. than W.T. mice (median and error, 95% CI). (E) Seizure duration (after-discharge, s) was shorter in GluA1 K.O. than in W.T. mice. Data are mean ± SEM, * $p < 0.05$.

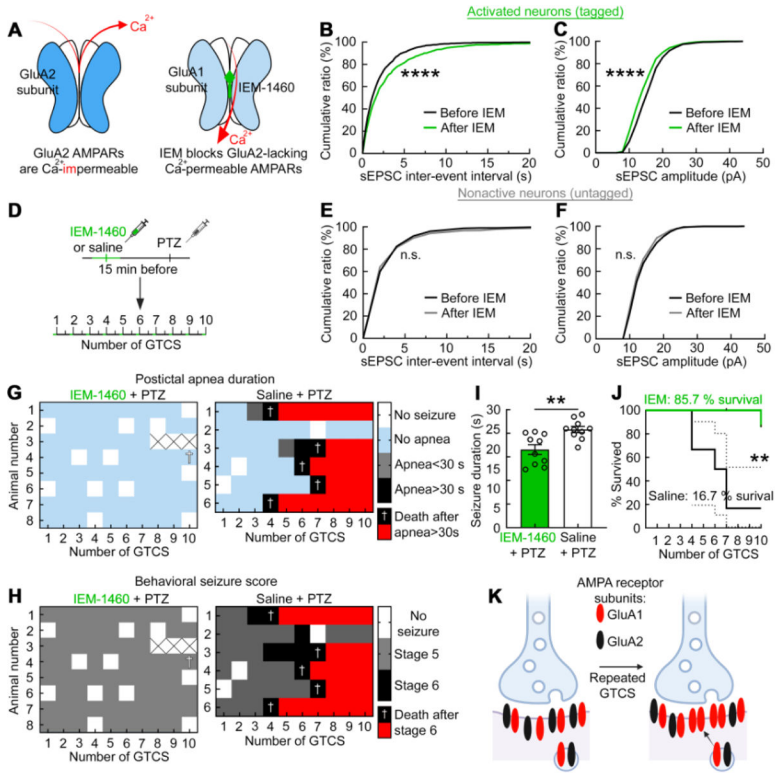

Fig. 6. Blockade of calcium-permeable AMPA receptors prevents postictal apnea and seizure-induced death.

(A) IEM-1460 blocks calcium-permeable AMPARs. (B) Cumulative ratio (%) of sEPSC inter-event intervals decreased after IEM (green) application (before is black) only in activated neurons. (C) Cumulative ratio (%) of sEPSC amplitudes decreased after IEM (green) application (before is black) only in activated neurons. (D) IEM-1460 or saline were injected i.p. 15 min before each PTZ injection every other day for a total of 10 seizures. (E,F) IEM application (grey) did not affect sEPSC inter-event interval frequency (e) or amplitude (f) in nonactive neurons. (G) Postictal apnea did not occur in IEM-treated mice. (Mice #3&4 died in a home cage without a seizure in between assigned PTZ injection days). (H) Behavioral seizures worsened with repetition in saline-injected mice but not in IEM treated. (I) Overall seizure duration in saline-injected mice was longer. (J) Kaplan-Meyer survival curve demonstrates more IEM-treated mice survived than saline injected. (K) We propose repeated seizures traffic the GluA1 subunit-containing AMPA receptors to synapses, and blocking this mechanism leads to better survival.